



# Enhancement of Open-Ended Tabular Pile Lateral Resistance with External Wings

Received 26 November 2021; Revised 27 December 2021; Accepted 27 December 2021

Ezzeldin K. Mohamed<sup>1</sup>  
Emad Helal<sup>2</sup>  
Eehab Khalil<sup>3</sup>

## Keywords

Open-Ended tabular pile,  
Lateral Resistance, Single pile  
foundation, Soil structure  
interaction, Pipe pile

## Abstract

The foundations for offshore wind turbines represent the main item either for cost or installation process, and the lateral resistance of tabular piles is the main factor for its design. Therefore, studies for consistent and efficient foundations have become essential for offshore wind turbines when using traditional mono-pile foundations under practical and environmental conditions. This research discusses the increase in the lateral behaviour of open tabular piles with the addition of external wings near the ground level with specific dimensions. Four wings were added to the exterior wall of the open-ended pipe pile at equal angles 90 degrees. The wings length varied from 0.25 to 0.5 of the pile diameters. Each wing length is studied with two depths of 1.25, and 2.5 pile diameter. The numerical analysis was verified with published results of centrifugal tests. The successive parametric study discussed the feasibility of the added wings. Inclusive, the resultant load direction was considered as changed between 0 to 45o with 5 degrees to the wing's orientation horizontally

## 1. Introduction

Wind energy has become the most promising green energy compared to traditional sources. The foundation of Offshore Wind Turbines (OWT) represents the predominant item for this structure type regarding both cost and installation procedure, especially when construction in zones of deeper seawater or when the increasing distance to shore [1], [2]. Also, the construction of the foundation represents the major number of materials and generates most of the CO<sub>2</sub> emissions in cement production [3]. Additionally, the new generation of wind turbines with larger capacities increases the difficulties of installation and cost when using traditional mono-pile foundations under practical and environmental conditions [4], [5]. Therefore, the traditional mono-pile foundation for OWTs may not be effective to provide an adequate efficient design considering various load cases and environmental conditions.

Arshi and Stone [6], [7] proposed a hybrid mono-pile-footing foundation concept, which consisted of a mono-pile attached to a bearing plate at the seabed, Figure 1. While previous studies were mainly involved in vertical loads, Arshi et al, investigated the behaviour of the proposed system under the effect of both vertical and lateral loadings. Several centrifuge tests were performed to

<sup>1</sup> Construction Research Institute, National water Research Center, Egypt

<sup>2</sup> October University for Modern Sciences and Arts (MSA), Egypt.

<sup>3</sup> Construction Research Institute, National water Research Center, Egypt.

study the behaviour of this system and an analytical solution was proposed to analyse its ultimate lateral bearing capacity. It was concluded that this proposed system considerably improves the lateral capacity of the mono-pile foundation by about three times compared to the traditional mono-pile system.

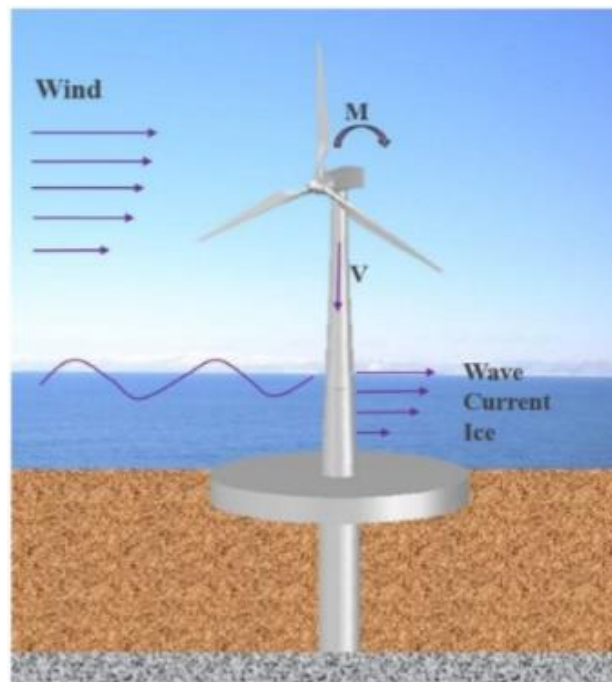


Figure 1 Schematic of OWT with hybrid monopile foundation

Lebane, et al., [8] continued investigation of the hybrid foundation system behaviour, concluding that the moment transferred to the mono-pile was reduced by the footing addition at the soil surface, and larger ultimate lateral resistance was obtained. In the hybrid mono-pile foundation system, a circular friction wheel is added at the seabed to provide additional resistance against both vertical and lateral loads in addition to overturning resistance; several studies adopted this system [12-16].

Wang, et al. [1], [8] investigated the behaviour of OWTs with the hybrid mono-pile foundation under service conditions and lateral cyclic loadings, by considering the wind, waves, and ice effects. A series of centrifuge tests were conducted to analyse these loading effect behaviours compared to the traditional mono-pile system. The results indicate that the hybrid foundation provides a larger cyclic capacity than the other foundation's types.

A series of centrifuge tests were performed to examine the feasibility of this new foundation system for OWTs in cohesive soil. Analytical methods were proposed to predict the ultimate bearing capacity and the cyclic response, which aims to provide design references for practical applications. It was concluded that the hybrid mono-pile foundation provides larger ultimate bearing capacities than the traditional mono-pile in clay. Adding a friction wheel improved pile moment resistance, and this system is effective in enhancing resistance to external loads, and the steel wheel is more effective than the gravel wheel [9], [22].

Wang, et al. [10]–[12] performed a series of centrifuge tests to study the mechanism of seismic response and liquefaction characteristics of this innovative foundation system using both steel and gravel friction wheels. It was concluded that the mono-pile foundation experiences a large tilt during the earthquake. The proposed hybrid mono-pile foundations achieve smaller lateral deformations, and the soil bearing capacity is improved. The restoring moment enhances the structural lateral stability. Where the steel wheel foundations tilt less than the gravel wheel foundations.

On the other hand, Wang, et al. [13],[14], [22] performed centrifuge tests to investigate the seismic response of suction bucket foundation under earthquake loading; for both dry and saturated soil conditions, Figure 2. The considered parameters are the bucket diameter, penetration depth, and modified buckets with inside partitions. It was found that soil underlying and near the bucket foundation showed a better ability to resist liquefaction, especially for saturated cases.

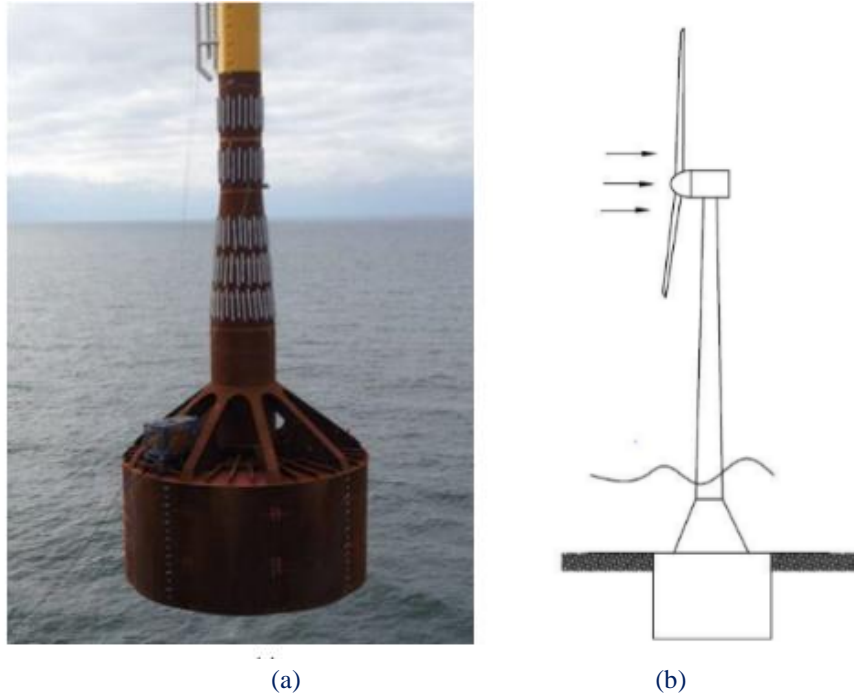


Figure 2 Offshore Wind Turbine with Suction Bucket Foundation

(a) the first suction bucket foundation installed in the UK; (b) schematic plot of suction bucket foundation for OWT

Additionally, Wang X, et al. [15] performed a series of centrifuge tests to investigate the bearing capacity of axially loaded mono-piles in the sand, and both open-ended and close-ended piles are tested considering service conditions such as loading rate, embedment depth, and the loading history. The tests indicate that the pile bearing capacity tends to increase with the initial penetration depth, and the stress state of soil greatly influences the pile behaviour. The tensile shaft friction is smaller compared to the compression test.

Li et al. [16][17], investigated the bearing behaviour of an innovative pipe pile with the addition of a restriction plate inside the pile, compared to the traditional system under both static and dynamic loads through a series of geotechnical tests. The proposed plates either having one hole or four holes with different pile diameters have been investigated, Figure 3. The design is based on the soil plug mechanism and the arching effect. The results indicated that the proposed system is efficient in enhancing the bearing capacity compared to the open-ended and close-ended pipe pile by intensifying the plug effect.

To understand the pile-soil interaction, researchers focused to measure the ultimate pile load rather than soil pile interaction pressure along with its depth as a function of load [18]. However, Trevor Smith. [19], compared the theories discussing the pressure surrounding piles. The assumption of stress linear distribution is far from reality, and the pressure devices used only to measure the head pressure which does not consider the significant shear to resist translation. The calculation of the pile laterally capacity based on the double differentiation of measured bending strain; that reaches 88% of the soil reaction from horizontal equilibrium, Figure 4. It could be concluded, that as the compressive pressure increases, the lateral resistance of the pile increases.

This research focuses on increasing the compressive pressure and increasing the pile projected area. Where the enhancement of the lateral pipe pile resistance depends on the increase of pile surface area, which reflects in an increase in frictional areas and increases the soil surface bearing and supporting soil passive pressure. The improvement depends on the pile lateral resistance using external wings to increase the effective passive stresses resist the pile lateral deformation.

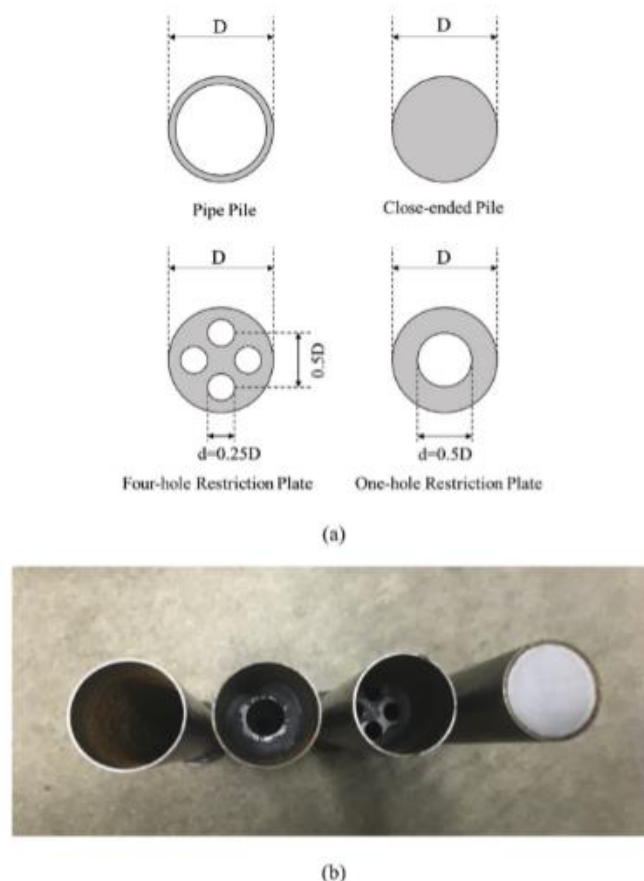


Figure 3 The different-shape restriction plates: (a) Schematic models, (b) Test Models [17]

## 2. Numerical verifications

The reference mono-pile foundation is based on the mono-pile foundation installed at Offshore Wind farm Emond and Zee. This reference pile had a 4.4 m diameter and has a wall thickness of  $1/80D$ , and an embedded pile length of about  $6D$ . A proposal for using shorter piles with a larger diameter maintaining a constant embedded length; where piles length to diameter ratio ( $L/D$ ) reaches 5 already installed for future farms and  $L/D$  ratio of 4.7 have been used at the British Lynn and Inner Dowsing Wind Farm. A prototype Pile had had a diameter of 2.20m, with an embedded pile length of 11 m and a wall thickness of 3 cm. A model has been scaled down and tested experimentally in a centrifuge test in TU-Delft [20]. The prototype is scaled to corresponding stiffness, where the pile young's modulus of 110 GPa compared to 210 GPa, and the wall thickness is doubled. Figure 5 shows a schematic cross-section for the pile and test setup. Verification models using FEA-DIANA software were developed and verified with the experimental tests' results.

A  $0.1 D$  horizontal static displacement was applied to simulate the real loading condition as displacement load; the test is displacement control with 0.5 mm/sec and the accuracy of test measurements of 0.1 mm. The forced displacement and the corresponding force measurements are applied at a height of 2.4 mm above the soil surface.

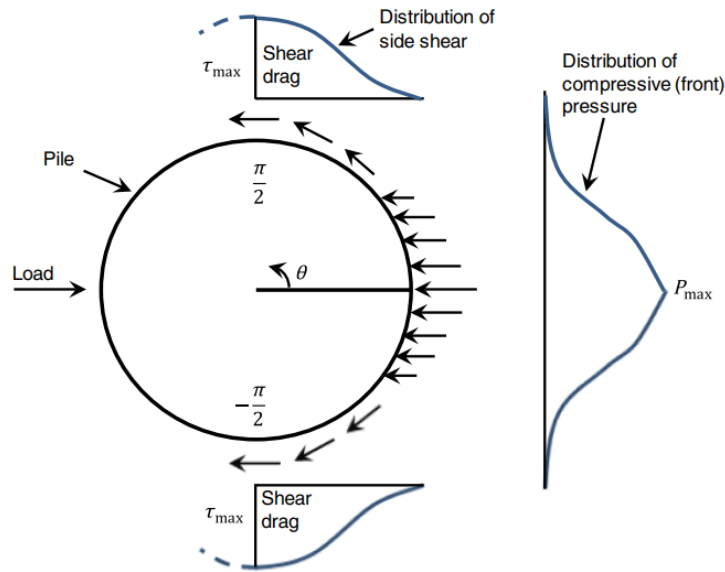


Figure 4 Soil-pile interaction stresses for laterally loaded piles at one depth [19]

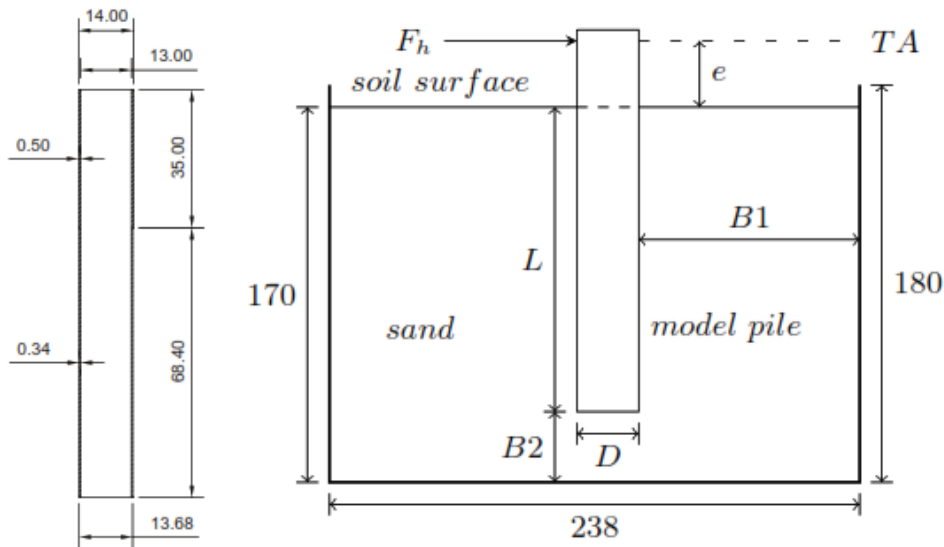


Figure 5 schematic cross-section of the pile and test setup (mm) [20]

### 3. Model discretization

The soil and pile were modelled as a quadratic solid element, Figure 6. An interface element has been placed between the pile and the surrounding soil to capture the non-tension allowed between the soil and steel pile. The mesh size for the pile and surrounding soil is 2 mm and increased far from the pile to the boundaries of the sandbox. The strongbox is modelled as fixed supports for the walls. Additionally, a composed beam is located at the centreline of the pile for integrating the resultant shear forces acting on the pile. Additionally, a composed straight-line base element; with a thickness equal to the diameter of the pile is defined to set bandwidth for the location of structural nodes to calculate forces and moments acting on the pile. As a guideline to obtain the values of the normal ( $K_n$ ) and tangential stiffness ( $K_t$ ) of interface elements, one can use the following expressions[21]:

$$K_n = \frac{100 \sim 1000 E}{L_e}, \quad K_t = \frac{K_n}{10 \sim 100}$$

Where;  $L_e$  is the average mesh element size; E: Young's moduli of the elements surrounding the interfaces.

The interface surface between the soil and the pile allows pile-soil separation and slippage. The reaction resultant load of the displacement was calculated at 2.4 mm above the soil surface. Based on the experimental work, the numerical model has been verified and validated with the experimental tests, where the static tests are the verification Key, as shown in the comparison between the load and displacement, Figure 7. The model was analysed in two steps, the first is geostatic stress surrounding the pile under gravity load, and the second step was the horizontal deformation applied on the pile considering loading sub-steps to ensure the convergence of the numerical. The comparison of lateral deformation between the centrifugal tests and the Finite element model showed a good agreement where the main concern is to be more conservative than the experimental work to underestimate the effectiveness of the proposed wing effectiveness.

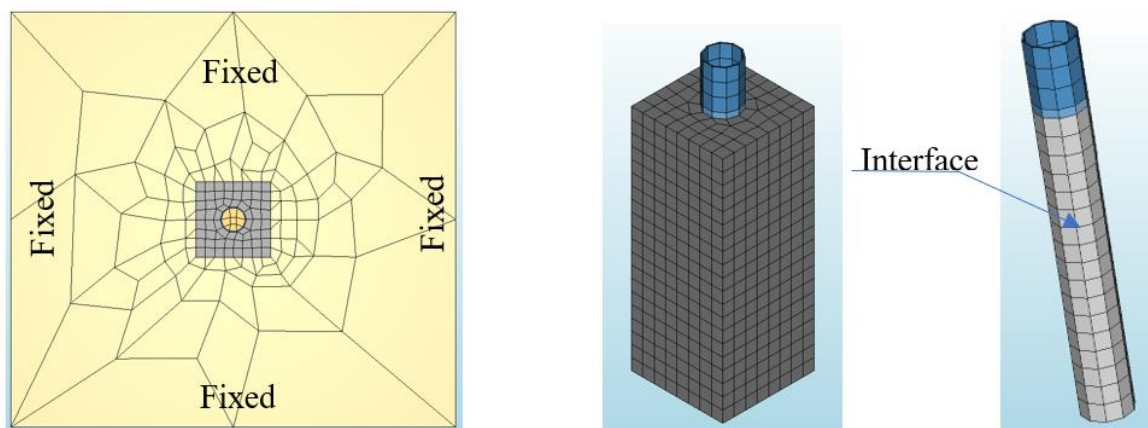


Figure 6 Model discretization (Mesh and Boundary conditions)

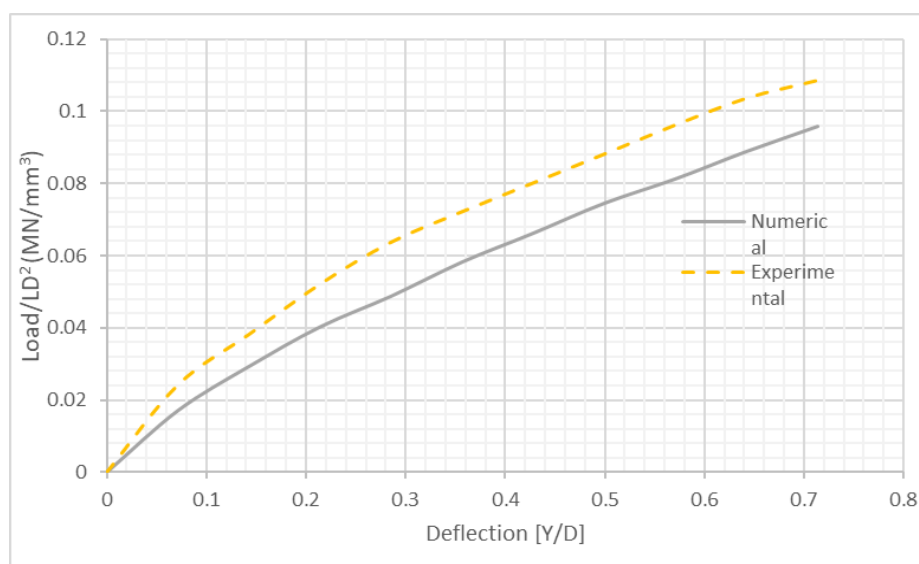


Figure 7 comparison between numerical and experimental tests [19]

#### 4. Parametric study

The main objective of this research is to increase the lateral load pile capacity by adding external wings, followed by a parametric study on wings dimensions. A traditional steel pipe pile is considered as a reference pile and has four wings around the pile at 90 degrees, where its widths were 0.25 D and 0.5 D. Also, the lengths of the added wings are 1.25 D, and 2.5D, Figure 8.

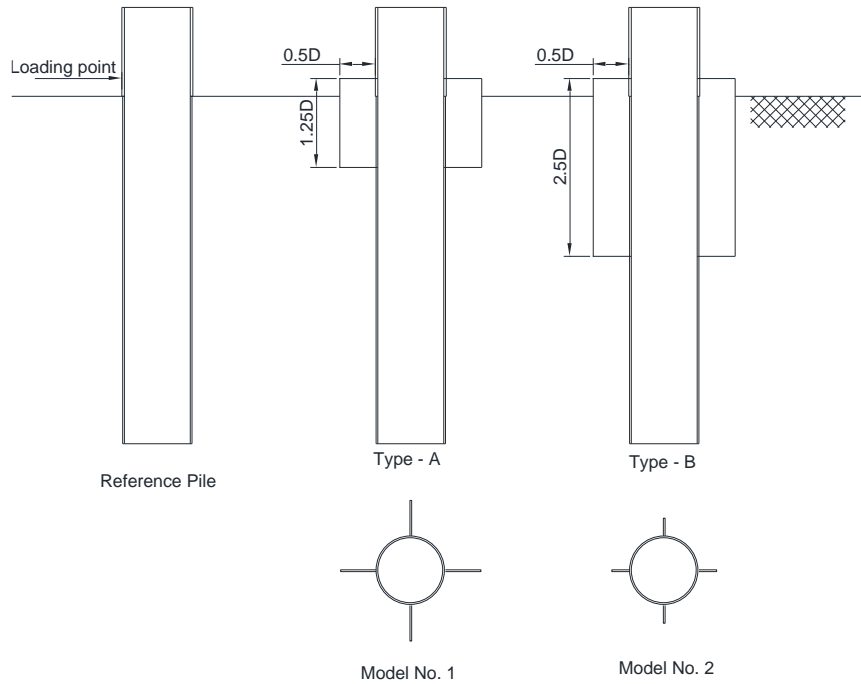


Figure 8 schematic sketch for the added wings

Table 1 parametric study

Model Name	Wing Width	Wing Length	Angle (Degree)
Reference	NA	NA	NA
A1	0.5 D	1.25 D	NA
A2	0.25 D	1.25D	NA
B1	0.5 D	2.5 D	NA
B2	0.25 D	2.5 D	0 ° to 45 ° (each 5°)

#### 5. Results and discussion

This section discusses the effectiveness of the proposed wings compared with a traditional pile in terms of lateral load and its corresponding deformation, maximum moment, and maximum shear.

##### 5.1 Load deflection curve

The added wings improved the lateral resistance of the pile where the soil resistance forces increased with the increase in the wing's dimensions. It increased four times the reference case for the 0.5 D wedges width and 2.5 D depth. As the wing width increase, the lateral resistance increases where it reached its maximum at the wing width equals half of the diameter,

Figure 9. The wings raise the soil pile interaction and increase the lateral resistance. Where, the increase of lateral resistance is a direct result of the pile projected area increase; where the area of

normal resistance increased by double and the shear resistance relatively decreased and mainly depend on the soil internal friction as it could be concluded from the changes of the bulb of stresses surrounding the pile. However, at lower values of lateral loads, the piles have approximately the same curve till the excitation of soil passive pressure.

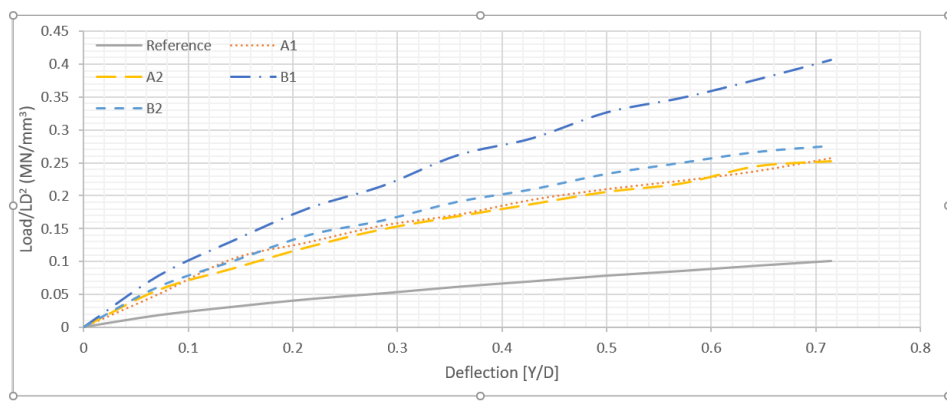


Figure 9 Load displacement for the studied cases

The interaction between soil and the pile is mainly normal resistance as Pile A1, where most of the resisting soil is within the projected area of the wings. On the other hand, by the decrease of the wings area, the soil around the back wing interaction is insignificant. And, by the increase of wings depth [B1, B2], the soil interaction around the pile increased and the ground displacement decreased. Where, the bulb of deformation around the pile decreased by the wings added for case A1 and decreased again by the increase of the wing's depth as in B1, Figure 10. The deformation bulb around the traditional pile was about 4D, and mainly at the opposite of the loading direction. By adding the wings, the deformation bulb decreased to 2D for pile A1, and extended to the loading direction, and its opposite direction. However, with the increase of wings depth [Pile B], the bulb of deformation increased at the opposite of loading direction to be 2.5 D and decreased in the direction perpendicular to the loading.

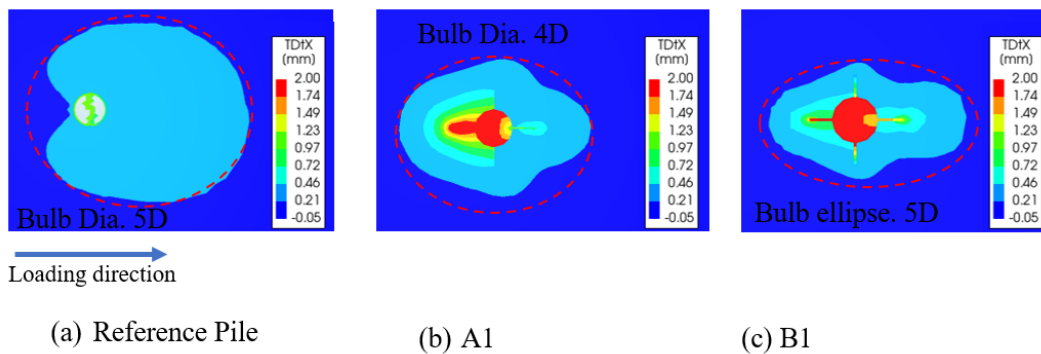


Figure 10 Deformation Bulb around piles.



## 5.2 Soil reaction

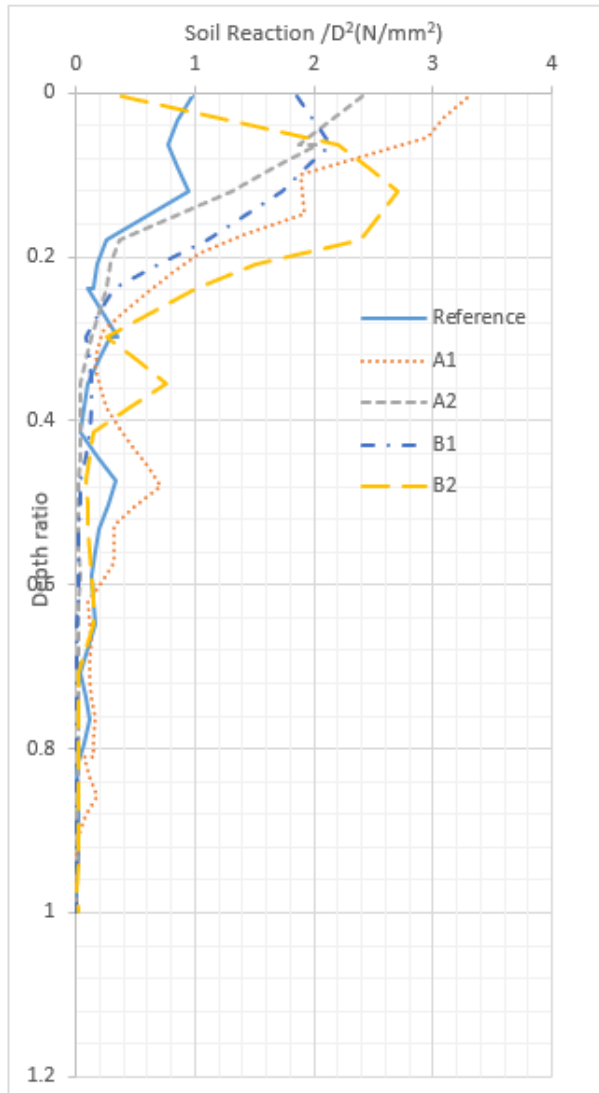


Figure 11 shows the soil reaction force diagram action on the pile as a resultant reaction, where it is calculated as a normalized reaction for forces acting on x, y, and z. Adding the wings, the soil reaction decreases. The shear forces acting on the pile because of the applied deformation decreases with the increase of the wings area, as Pile B2 is the lowest shear force where the wing width is 0.5 D and length is 2.5 D compared with A2 (0.25 D width, and 1.25 length). Moreover, as load angle increased the shear forces acting on the pile decreases with respect to the contribution of the perpendicular wings.

Adding the wings, the soil reaction increases, where the main resistance component is the normal resistance of the soil. For type A piles, the soil resistance increases near the ground level, as it was three times, and two times for piles A1, and A2 respectively. On the other hand, as the wings length increases, the soil resistance near the ground decreases due to the increase of wings anchoring

length, which makes the soil resistance relatively distributed along the length of the wings,

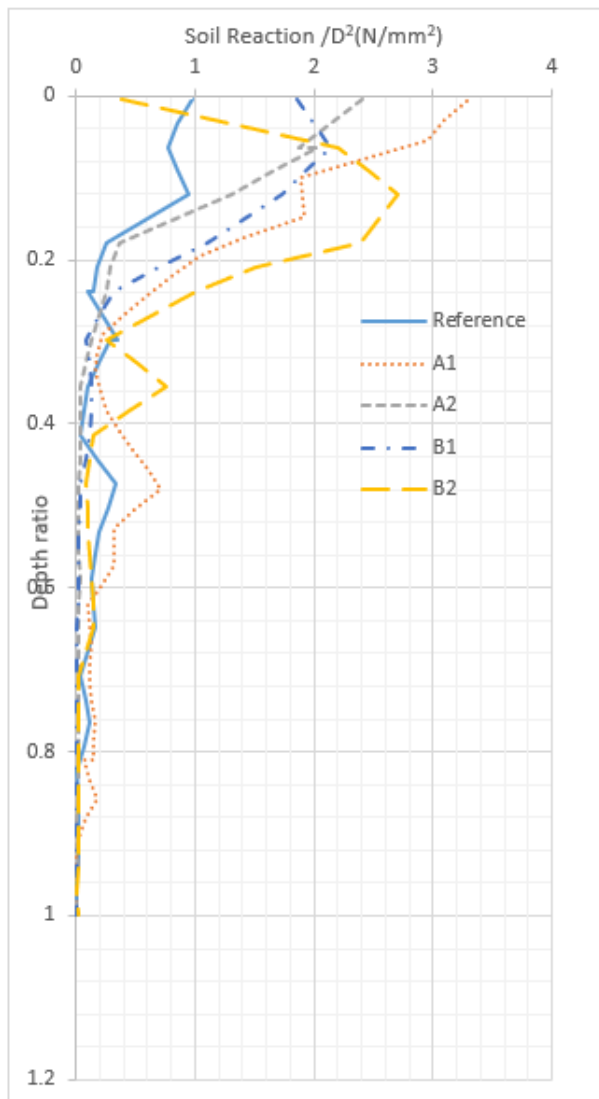


Figure 11. For shallow wings' depth, the soil resistance stresses are concentrated on the upper edge of the wing with relatively low stresses elsewhere with depth. For deep wings, the soil resistance is enhanced with some increase of the total force but with relative distribution of soil stresses along its depth.

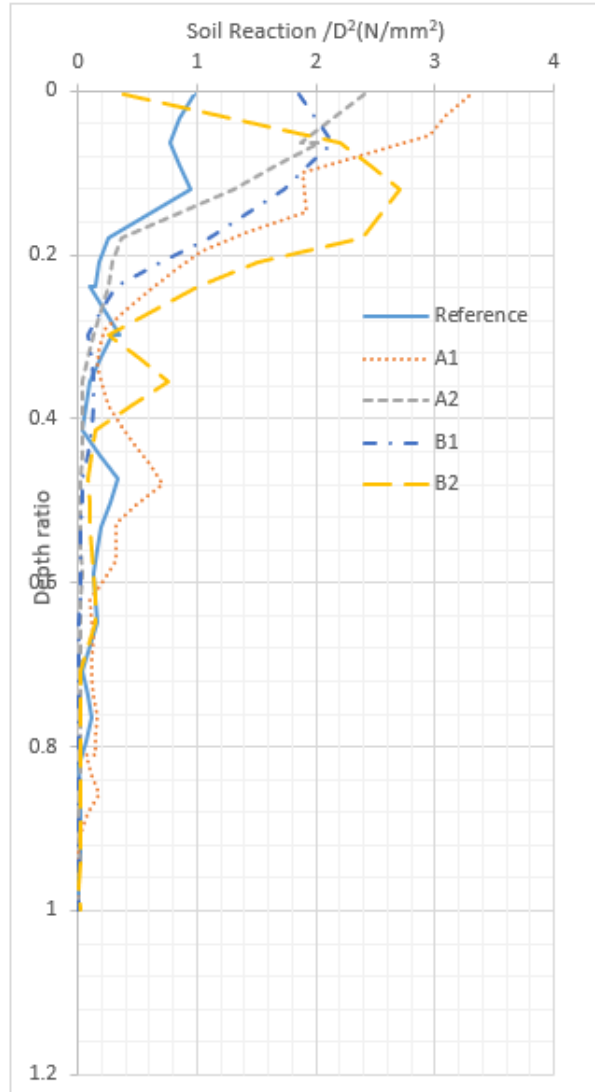


Figure 11 Soil reaction diagram acting on the pile

### 5.3 Resultant Load orientation

The practical applied loads are not fixed in one direction and change according to load resultant direction. It was suggested to change the loading direction between angles of  $0^\circ$  to  $45^\circ$  degrees with an increment of  $5^\circ$  degrees. As the results of Pile [B2] showed good improvement in the lateral resistance, it was considered to study the load orientation and its effect on the wings. By the load orientation, the ground displacement increased, and the corresponding load resistance increases, because of the pile and wings projection area changes, where its relatively increases, but the orientation angle affects the soil- pile interaction. The wings act as a sliding surface with respect to the loading angle, instead of bearing surfaces for the loading angle  $0^\circ$ . The maximum load was at angle  $35^\circ$  where the capacity load increased by 25% from the perpendicular load. However, at the angle  $5^\circ$ , the capacity load resistance decreased by 15% from the perpendicular load, Figures 13, 14, and 15.

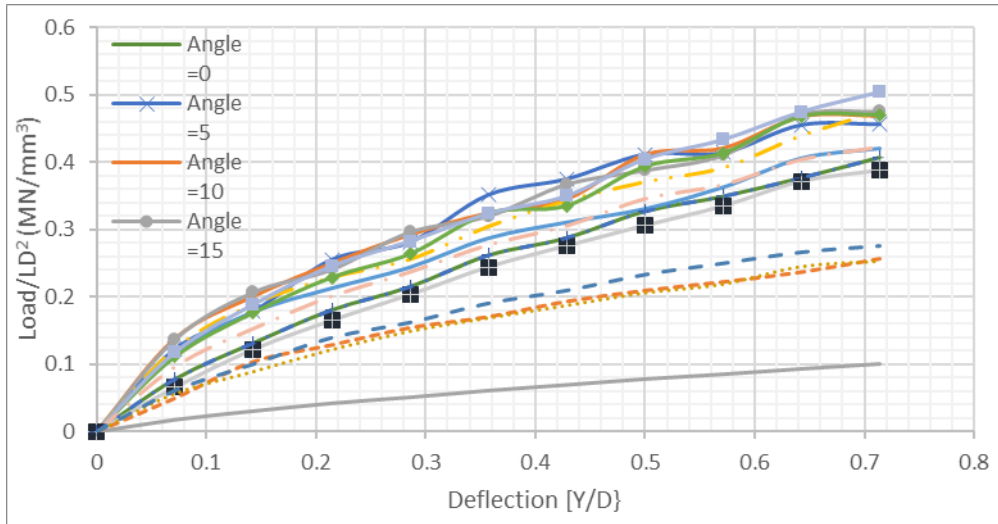


Figure 12 Load displacement for different load orientations.

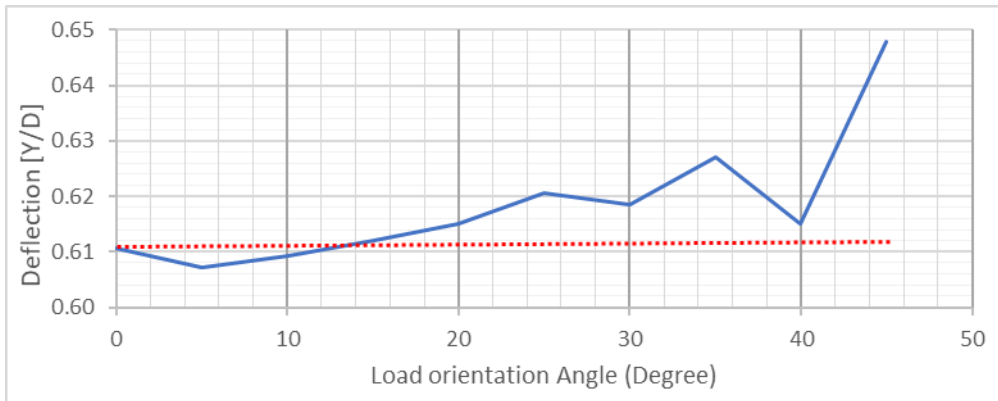
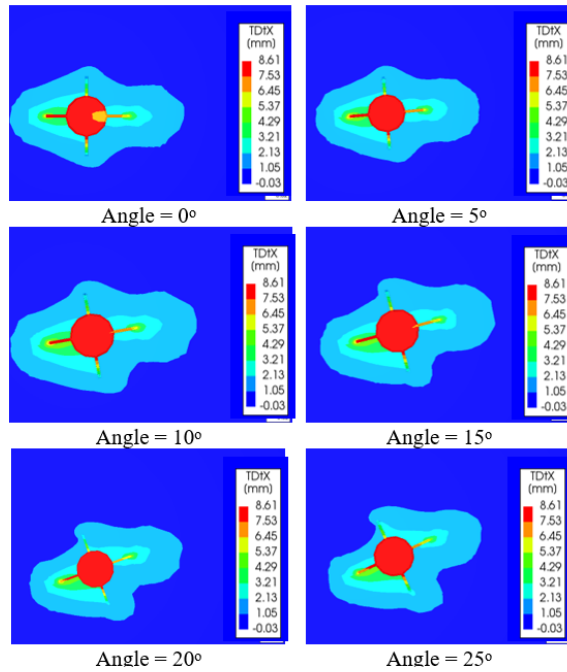


Figure 13 Ground displacement for different load orientations.



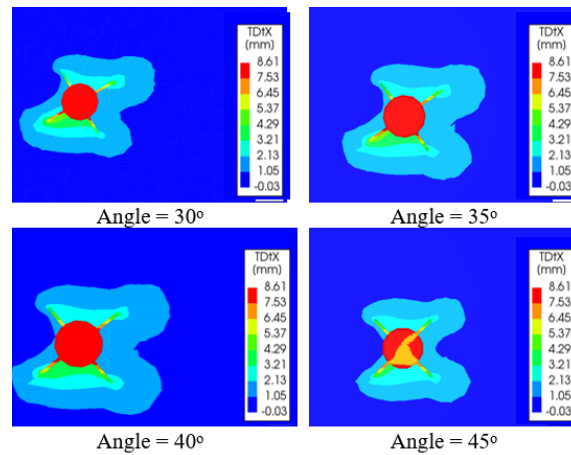


Figure 14 Deformation Bulb around the pile for the different load orientations.

## 6. Conclusions

The tabular piles are widely used especially for wind turbines and their lateral resistance is a major factor in its design as static and cyclic load. This study focused on the enhancement of the tabular pile resistance using exterior wings near the ground surface. The parametric study focuses on the width and the length of the wings, which varied from 0.25 D to 0.5 D for the width, and 1.25 D, 2.5 D for the length. The computed lateral displacement of the pile with depth for the proposed wings, where the wings resist the pile deformation horizontally but where it reaches four times the reference pile under the maximum lateral load. The increase of the soil resistance is proposed to be a result of increasing the projection area of the pile which excites more passive pressure resisting the pile lateral deformation.

Generally, the addition of the wings increased the pile lateral resistance which reaches 4 times the traditional tabular pile by adding wings of 0.5D width and 2.5D length. And 2.5 times of the reference pile for 0.5D width and 1.25D length. In conclusion, as the width and depth of the wings increase the resistance forces increases, and lateral deformation decreases. In addition, the change of the resultant load direction has an insignificant effect on the pile lateral resistance. However, it decreases by 5% in the case of 45° rotation of the resultant load, and the ground displacement is increased by the increase of the load rotation angle.

## References

- [1] M.M. Al-Nasra, I.A. Duweib, A.S. Najmi, The Use of Pyramid Swimmer Bars as Punching Shear Reinforcement in Reinforced Concrete Flat Slabs, *J. Civ. Eng. Res.* 2013 (2013) 75–80. <https://doi.org/10.5923/j.jce.20130302.02>.
- [2] Al-Nasra, the Use of Swimmer Bars as Shear Reinforcement in Reinforced Concrete Beam, *Am. J. Eng. Appl. Sci.* 6 (2013) 87–94. <https://doi.org/10.3844/ajeassp.2013.87.94>.
- [3] P. Saravanakumar, A. Govindaraj, Influence of vertical and inclined shear reinforcement on shear cracking behavior in reinforced concrete beams, *Int. J. Civ. Eng. Technol.* 7 (2016) 602–610.
- [4] M. AL NASRA, Investigating Alternatives in Shear Reinforcements in the Reinforced Concrete Beams, (2015) 27–31. <https://doi.org/10.15224/978-1-63248-070-5-45>.
- [5] N.A.A. Hamid, the use of horizontal and inclined bars as shear reinforcement, *Use Horiz. Incl. Bars As Shear Reinf.* (2005) 131.
- [6] ACI Committee 318, *Building Code Requirements for Structural Concrete*, 2014.
- [7] E. (203-2017)., Egyptian Code of Practice for Design and Construction of [1] X. Wang, X. Zeng, J. Li, X. Yang, and H. Wang, “A review on recent advancements of substructures for offshore wind

- turbines,” *Energy Convers. Manag.*, vol. 158, pp. 103–119, 2018.
- [8] EWEA, “The European offshore wind industry key statistics report 2015,” ... — *Doc. ...*, no. January, pp. 1–31, 2016.
- [9] M. M. Savino, R. Manzini, V. Della Selva, and R. Accorsi, “A new model for environmental and economic evaluation of renewable energy systems: The case of wind turbines,” *Appl. Energy*, vol. 189, pp. 739–752, 2017.
- [10] Q. Li, Y. Kamada, T. Maeda, J. Murata, K. Iida, and Y. Okumura, “Fundamental study on aerodynamic force of floating offshore wind turbine with cyclic pitch mechanism,” *Energy*, vol. 99, pp. 20–31, 2016.
- [11] A. Pacheco, E. Gorbeña, C. Sequeira, and S. Jerez, “An evaluation of offshore wind power production by floatable systems: A case study from SW Portugal,” *Energy*, vol. 131, pp. 239–250, 2017.
- [12] H. S. Arshi *et al.*, “Modelling of monopile-footing foundation system for offshore structures in cohesionless soils,” *18th Int. Conf. Soil Mech. Geotech. Eng. Challenges Innov. Geotech. ICSMGE 2013*, vol. 3, no. September, pp. 2307–2310, 2013.
- [13] S. Arshi and K. Stone, “An investigation of a rock socketed pile with an integral bearing plate founded over weak rock Étude d ’ une pile avec une plaque encastrée dans une roche molle,” *Geotech. Eng.*, no. August 2015, pp. 705–710, 2011.
- [14] B. M. Lehane, B. Pedram, J. A. Doherty, and W. Powrie, “Improved Performance of Monopiles When Combined with Footings for Tower Foundations in Sand,” *J. Geotech. Geoenvironmental Eng.*, vol. 140, no. 7, p. 04014027, 2014.
- [15] X. Wang, X. Zeng, X. Li, and J. Li, “Investigation on offshore wind turbine with an innovative hybrid monopile foundation: An experimental based study,” *Renew. Energy*, vol. 132, pp. 129–141, 2019.
- [16] X. Wang, X. Zeng, X. Yang, and J. Li, “Seismic response of offshore wind turbine with hybrid monopile foundation based on centrifuge modeling,” *Appl. Energy*, vol. 235, pp. 1335–1350, 2019.
- [17] X. Wang, X. Zeng, J. Li, and X. Yang, “Lateral bearing capacity of hybrid monopile-friction wheel foundation for offshore wind turbines by centrifuge modeling,” *Ocean Eng.*, vol. 148, pp. 182–192, 2018.
- [18] X. Wang, X. Zeng, X. Li, and J. Li, “Liquefaction characteristics of offshore wind turbine with hybrid monopile foundation via centrifuge modeling,” *Renew. Energy*, vol. 145, pp. 2358–2372, 2020.
- [19] X. Wang, X. Yang, and X. Zeng, “Seismic Centrifuge Modelling of Suction Bucket Foundation for Offshore Wind Turbine,” *Ocean Eng.*, vol. 141, pp. 295–307, 2017.
- [20] H. S. Arshi *et al.*, “Modelling of monopile-footing foundation system for offshore structures in cohesionless soils,” *Renew. Energy*, vol. 235, no. 3, pp. 1335–1350, 2019.
- [21] X. Wang, X. Zeng, and J. Li, *Assessment of bearing capacity of axially loaded monopiles based on centrifuge tests*, vol. 167. 2018.
- [22] B. M. Lehane *et al.*, “Seismic response of offshore wind turbine with hybrid monopile foundation based on centrifuge modeling,” *Appl. Energy*, vol. 158, no. April, pp. 1–28, 2011.
- [23] J. Li, X. Wang, Y. Guo, and X. B. Yu, “The loading behavior of innovative monopile foundations for offshore wind turbine based on centrifuge experiments,” *Renew. Energy*, vol. 152, pp. 1109–1120, 2020.
- [24] M. Iftekharuzzaman and B. C. Hawlader, “Numerical modeling of lateral response of long flexible piles in sand,” *Geotech. Eng.*, vol. 44, no. 3, pp. 25–31, 2013.
- [25] T. D. Smith, “Pile horizontal soil modulus values,” *J. Geotech. Eng.*, vol. 113, no. 9, pp. 1040–1044, 1987.
- [26] E. A. Alderlieste, “Experimental Modelling of Lateral Loads on Large Diameter Mono-Pile Foundations in Sand,” *TU Delft*, vol. 138, no. April, pp. 1–28, 2011.
- [27] T. N. O. Diana, “User ’ s Manual Material Library,” 2018.
- [28] X. Wang, X. Zeng, X. Li, J. Li, Feasibility Study of Offshore Wind Turbines with Hybrid Monopile Foundation Based on Centrifuge Modeling, *App. Energy* 209, 2018, 127 – 139.

## تحسين المقاومة العرضية للخوازيق الأنبوبية بإضافة دعائم خارجية

### الملخص:

يناقش هذا البحث تحسين سلوك الخوازيق الأنبوبية تحت تأثير الاحمال الافقية بإضافة دعائم بأبعاد محددة على محيط الخازوق الخارجي وعلى عمق قريب نسبيا من سطح الأرض. وقد تم تجربة اضافة ٤ دعائم عمودية على السطح الخارجي للخازوق الأنبوبي المفتوح. وتم تطبيق أطوال مختلفة للدعائم (0.25 – 05) من قطر الخازوق، وكذلك تم تجربة تطبيق أعماق مختلفة للدعائم (1.25 – 2.5) مرة قطر الخازوق. وقد تمت معايرة النموذج العددي بنتائج اختبار الطرد المركزي، وبناءا عليه فقد تم مناقشة كفاءة هذا المقترح بإضافة الدعائم للخازوق وذلك باستخدام حالات متعددة في الدراسة للمتغيرات المختلفة. وأخيرا فقد تمت دراسة تأثير تغير اتجاه الحمل بالنسبة للاتجاه الأفقي لوضعية الدعائم المضافة وذلك بتغيير زاوية تأثير اتجاه الحمل من (0 – 45) درجة بمعدل تغير تدريجي ٥ درجات.

**الكلمات الدالة:** الخوازيق الأنبوبية المفتوحة – المقاومة العرضية – أساسات الخازوق المفرد – التأثير المتبادل للتربة مع الخازوق – الخوازيق الحديد المفرغة